JOURNAL OF Materials CHEMISTRY

Preparation of lead hydroxyapatite particles using acetamide

Akemi Yasukawa,* Takeshi Kunimoto, Kaori Kamiuchi, Kazuhiko Kandori and Tatsuo Ishikawa

School of Chemistry, Osaka University of Education, Asahigaoka 4-698-1, Kashiwara-shi, Osaka 582–8582, Japan. E-mail: yasukawa@cc.osaka-kyoiku.ac.jp

Received 28th January 1999, Accepted 21st May 1999

Lead hydroxyapatite (PbHAP) particles were prepared by a homogeneous precipitation reaction of $Pb(NO_3)_2$ and $(NH_4)_2HPO_4$ using acetamide (AA) in aqueous media. The particles obtained under different conditions were examined by various methods, including XRD, FTIR, SEM, ICP, TG–DTA and N_2 adsorption. The crystal phase of the products depended on the concentration of AA ([AA]) and the ageing period (t_a). Large highly crystalline needle-like PbHAP particles were formed by ageing at $[AA]=0.4$–$1.6\ mol\ dm^{-3}$ and $t_a \geq 1$ day. At $[AA] \geq 3.2\ mol\ dm^{-3}$ a mixture of PbHAP and α-$Pb_3(PO_4)_2$ was generated. The transformation of α-$Pb_3(PO_4)_2$ to PbHAP in solution at $[AA] \geq 3.2\ mol\ dm^{-3}$ was hindered by CH_3COOH, produced by hydrolysis of AA.

Introduction

Calcium hydroxyapatite [$Ca_{10}(PO_4)_6(OH)_2$, designated as CaHAP] is a primary constituent of vertebral animals' hard tissues and synthetic CaHAP has attracted attention due to its utility in the fields of bioceramics, chromatographic adsorbents and acid and base catalysts, among others. It has been established that the Ca^{2+} sites of CaHAP can be replaced by various divalent cations such as Sr^{2+}, Ba^{2+}, Pb^{2+}, Cd^{2+}, *etc.*[1] The exchange of Ca^{2+} ions in CaHAP with noxious Pb^{2+} ions is an interesting subject in medical and environmental sciences. It has been reported that lead–calcium hydroxyapatite (PbCaHAP) catalyzes oxidative dehydrogenation of methane to carbon oxides and hydrogen better than CaHAP.[2] Hence, lead hydroxyapatite (PbHAP), having Pb^{2+} ions in all the cation sites of hydroxyapatite (HAP), is also expected to be a better catalyst than the other HAPs. PbHAP particles have previously been synthesized by many investigators *via* hydrothermal[3–5] and precipitation[6–9] methods. Engel *et al.* prepared PbHAP hydrothermally from $Pb_{10}(PO_4)_6O$ at 425 °C under 1000 atm.[3] Blakeslee and Condrate[3] synthesized PbHAP by two methods; a hydrothermal treatment of $Pb_{10}(PO_4)_6O$ at 300 °C and a precipitation reaction of $Pb(NO_3)_2$ and $(NH_4)_2HPO_4$ followed by hydrothermal treatment at 300 °C. Crystalline particles with a size less than 300 μm were obtained by the latter method.[4] Negas *et al.* prepared PbHAP hydrothermally from PbO and $NH_4H_2PO_4$ at room temperature, 300, 600 and 900 °C.[5] On the other hand, Narasaraju *et al.* obtained PbHAP particles with a size of *ca.* 50 × 250 nm by a precipitation reaction of $Pb(NO_3)_2$ and $(NH_4)_2HPO_4$ at pH 12 and 37 °C.[6] Moreover, PbHAP particles were produced from a solution containing $PbHPO_4$ and NaOH which had been aged at 40 °C for 7 days,[7] from solutions containing $Pb(CH_3COO)_2$ and various monohydrogen phosphates aged at 100 °C for 4–24 h[8] and from solutions containing basic $Pb(NO_3)_2$ and H_3PO_4.[9]

We have previously prepared needle-like CaHAP particles by a homogeneous precipitation method using acetamide (CH_3CONH_2, designated as AA),[10] where AA is hydrolyzed at an elevated temperature according to the following reaction [eqn. (1)].

$$CH_3CONH_2 + H_2O \rightarrow CH_3COOH + NH_3 \qquad (1)$$

The resultant NH_3 raises the solution pH to yield highly crystalline CaHAP particles. The materials formed with AA contain few carbonate ions, in contrast to the preparation using urea, widely employed as a homogeneous precipitation agent. As AA evolves no gaseous decomposition products, it is appropriate for the synthesis in a closed system. Furthermore, because of the slow hydrolysis of AA, the formed particles are much larger and better crystallized than those prepared by the documented methods without AA.[11–13]

In the present study, we turn our attention to PbHAP preparation by a homogeneous precipitation method using AA. The structure of the products was explored by various techniques. To ascertain the best conditions for PbHAP preparation, the relationship between synthesis conditions and crystal phases of the products was determined. Based on the results obtained, the formation mechanism of PbHAP is discussed.

Experimental

Materials

25 cm^3 of a 0.5 $mol\ dm^{-3}$ $Pb(NO_3)_2$ solution was added to 12.5 cm^3 of a 2 $mol\ dm^{-3}$ NH_4NO_3 buffer solution. To this solution were added different amounts of AA ranging from 0.05 to 1.2 mol and 12.5 cm^3 of a 0.6 $mol\ dm^{-3}$ $(NH_4)_2HPO_4$ solution.[14] The Pb/P molar ratio in the resulting solution was 1.67; equivalent to the stoichiometric ratio of PbHAP. The resulting white precipitates were a mixture of $PbHPO_4$ and α-$Pb_3(PO_4)_2$ as confirmed by X-ray diffraction (JCPDS 29–773 and 25–1394, respectively). The precipitates were redissolved by adding 1 $mol\ dm^{-3}$ HNO_3 solution to prepare large particles by homogeneous precipitation. Then the solution volume was adjusted to 250 cm^3 by adding water. The solutions obtained, which contained 0.05 $mol\ dm^{-3}$ $Pb(NO_3)_2$, 0.10 $mol\ dm^{-3}$ NH_4NO_3, 0.20–4.80 $mol\ dm^{-3}$ AA, 0.03 $mol\ dm^{-3}$ $(NH_4)_2HPO_4$ and 0.23–0.47 $mol\ dm^{-3}$ HNO_3, were aged in 500 cm^3 screw-capped polypropylene vessels at 100 °C for 6 h–30 days. The supernatant pH at room temperature was measured after the ageing. The precipitates formed were filtered off, washed with water and finally dried in an air oven at 70 °C for 16 h. All the deionized, distilled water used was further purified by boiling under an N_2 atmosphere to remove CO_2 and all the chemicals used were guaranteed reagent grade and used as received.

Characterization

The materials synthesized were characterized by the following conventional techniques. Powder X-ray diffraction (XRD) was carried out with a Rigaku Geigerflex 2013 diffractometer using Ni-filtered Cu-Kα radiation (30 kV and 15 mA). The particle morphology was observed with a scanning electron microscope (SEM, JEOL JSM-840A) and a transmission electron microscope (TEM, JEOL 1200 EX). Transmission infrared spectra were taken by the KBr method using a Fourier transform infrared spectrometer (FTIR, Nicolet Protégé 460). Pb content was determined using an induced coupled plasma spectrometer (ICP, Seiko SPS 1200 AR), by first dissolving the sample in HNO_3, and PO_4^{3-} was assayed by the molybdenum blue method after dissolving the sample in HCl solution. The specific surface areas were evaluated by fitting the BET equation to the N_2 adsorption isotherms recorded by a computer-aided automatic volumetric apparatus at the boiling point of nitrogen. Prior to the adsorption, the samples were heated at 300 °C under 10^{-3} Torr for 2 h. Simultaneous thermogravimetry and differential thermal analyses (TG–DTA) were performed using a Seiko SSC 5200 thermoanalyzer in air at a heating rate of 5 °C $\min^{-1}$.

Results and discussion

Crystal structure

In order to examine the effect of AA concentration (abbreviated to [AA]) on PbHAP formation, particles were prepared from solutions with [AA] from 0.2 to 4.8 mol dm^{-3}. The ageing period (t_a) was 18 days. XRD patterns for the particles obtained are shown in Fig. 1. Pattern (a) of the product at the low [AA] of 0.2 mol dm^{-3} shows high crystallinity and diffraction peaks due to $PbHPO_4$ (JCPDS 29–773), marked with open squares, although a weak unknown peak is detected at $2\theta = 24.3°$ shown by a solid square. At [AA] = 0.4–2.4 mol dm^{-3}, well crystallized PbHAP particles (JCPDS 24–586) were generated as shown in patterns (b) and (c). At [AA] $\geq$ 3.2 mol dm^{-3}, a weak peak (open triangle) due to α-$Pb_3(PO_4)_2$ (JCPDS 25–1394) appears at $2\theta = 28.6°$ besides the PbHAP peaks [patterns (d) and (e)]. The intensities of the PbHAP peak are not affected by [AA] [patterns (b)–(e)].

To examine the effect of t_a, particles were prepared at [AA] = 2.4 mol dm^{-3} with $t_a = 6$ h–30 days. XRD patterns of the resultant products are shown in Fig. 2. The XRD pattern of the material formed at $t_a = 6$ h is characteristic of a mixture of PbHAP, α-$Pb_3(PO_4)_2$ and $PbHPO_4$ as seen in pattern (a). The product at $t_a = 1$–10 days is a mixture of PbHAP and α-$Pb_3(PO_4)_2$ [patterns (b) and (c)] and pure PbHAP is formed when $t_a \geq 14$ days [patterns (d) and (e)]. All the products are highly crystalline and their XRD peak intensities are essentially unchanged by ageing at $t_a \geq 1$ day. This indicates that a mixture of PbHAP, α-$Pb_3(PO_4)_2$ and $PbHPO_4$ transforms to a mixture of PbHAP and α-$Pb_3(PO_4)_2$, and finally to PbHAP as the ageing progresses. The unit cell dimensions *a* and *c* of all the obtained PbHAP particles, calculated from the XRD peaks due to (300) and (004) peaks, were 0.983–0.986 and 0.743–0.745 nm, respectively. These values agree with the dimensions *a* and *c* published for PbHAP (JCPDS 24–586) of 0.986 and 0.743 nm, respectively, and do not change with [AA] or t_a. We evaluated the crystallite sizes of the particles from the half-height width of XRD peaks shown in Fig. 1 and 2 using the Scherrer equation.[15] All the values obtained were larger than 100 nm, indicating that all the PbHAP particles produced are highly crystalline.

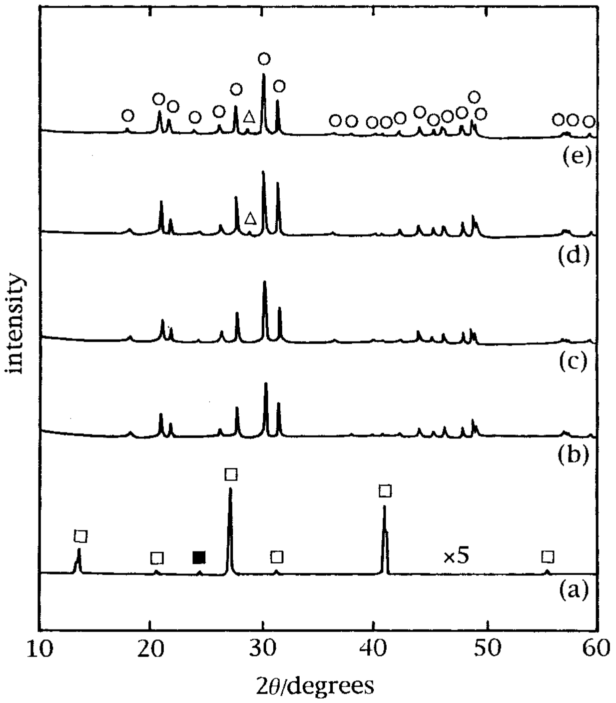

Fig. 1 XRD patterns of the materials formed at $t_a = 18$ days and different [AA]: (a) 0.2, (b) 0.4, (c) 2.4, (d) 3.2, (e) 4.8 mol dm^{-3}. (○) PbHAP, (△) α-$Pb_3(PO_4)_2$, (□) $PbHPO_4$, (■) unknown. XRD pattern (a) is reduced to 20%.

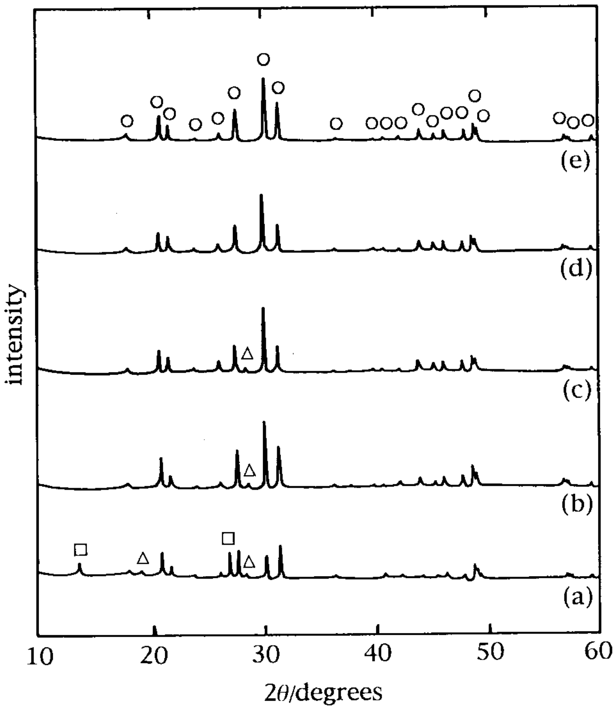

Fig. 2 XRD patterns of the materials formed at [AA] = 2.4 mol dm^{-3} and different t_a: (a) 6 h, (b) 1 day, (c) 10 days, (d) 14 days, (e) 30 days. (○) PbHAP, (△) α-$Pb_3(PO_4)_2$, (□) $PbHPO_4$.

Morphology

Fig. 3 displays SEM images of the particles prepared by ageing at various [AA] with $t_a = 18$ days. The $PbHPO_4$ particles formed at [AA] = 0.2 mol dm^{-3} [picture (a)] are large and plate-like with dimensions of 0.4 × 5 mm. Small needle-like particles can be seen on the surface of the large plates, but have not been identified at present. The large needle-like particles formed at [AA] = 0.4–2.4 mol dm^{-3} [pictures (b)–(d)] were confirmed as PbHAP by XRD as described above. It is noteworthy that hexagonal columnar PbHAP particles larger than 40 μm in width are generated at [AA] = 0.4 mol dm^{-3} [picture (b)] and the size of the longest PbHAP particle prepared at [AA] = 0.8 mol dm^{-3} is 10 × 400 μm [picture (c)]. To our knowledge, such large PbHAP particles have not been prepared previously by a wet method at low temperature (100 °C) under atmospheric pressure. To compare the syntheses with and without AA, we prepared PbHAP particles using NH_3 (aq) solutions instead of AA to adjust the solution pH to 8.5 and aged the products at 100 °C with $t_a = 2$ days. A

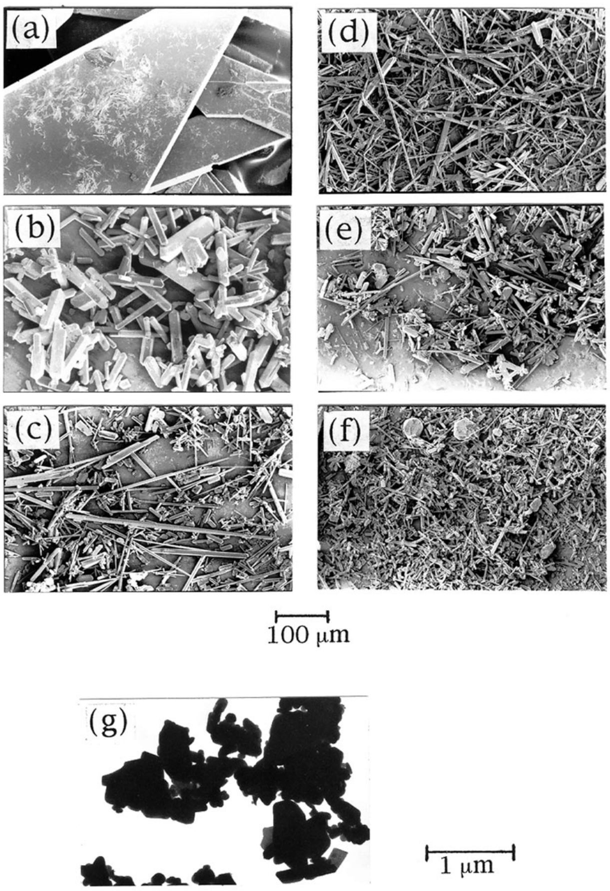

Fig. 3 SEM pictures of the materials formed at $t_a = 18$ days and different [AA] (a)–(f) and TEM picture of the particles formed with NH_3(aq) and $t_a = 2$ days (g). [AA]: (a) 0.2, (b) 0.4, (c) 0.8, (d) 2.4, (e) 3.2, (f) 4.8 mol dm^{-3}.

TEM image of the PbHAP particles thus obtained is shown in picture (g) in Fig. 3. All the PbHAP particles prepared with AA are considerably larger and more crystalline than those prepared using NH_3 (aq), whose sizes are 50–700 nm. In pictures (e) and (f) of the products formed at [AA] $\geq$ 3.2 mol dm^{-3}, irregularly shaped particles are mixed with needle-like particles; these are identified as α-$Pb_3(PO_4)_2$ and PbHAP, respectively. The needle-like PbHAP particles become smaller with increasing [AA] from 0.8 to 4.8 mol dm^{-3} as shown in pictures (c)–(f). This can be rationalized as resulting from a larger number of nuclei being produced at high [AA], leading to the formation of smaller particles.

To determine the effect of t_a on the morphology of the PbHAP particles, SEM pictures of the particles formed after ageing solutions at [AA] = 2.4 mol dm^{-3} and different t_a were taken and are shown in Fig. 4. Large needle-like particles are found in all the SEM pictures. In pictures (a) and (b) of the particles prepared at $t_a \leq 6$ days, irregularly shaped particles are found besides the needle-like PbHAP particles. The products at $t_a \geq 14$ days [pictures (c) and (d)] are needle-like particles only. Conditions of $t_a = 6$ h and 6 days gave mixtures of PbHAP, α-$Pb_3(PO_4)_2$ and $PbHPO_4$ and of PbHAP and α-$Pb_3(PO_4)_2$, respectively, as verified from the XRD patterns discussed in the crystal structure section. Thus the needle-like particles are identified as PbHAP and the other irregularly shaped ones as α-$Pb_3(PO_4)_2$ and $PbHPO_4$. Although the morphology change from irregular to needle-like with progress of ageing was detected, no marked crystal growth of the needle-like PbHAP particles could be observed at $t_a \geq 1$ day.

IR spectra

To get information on the short range structures of the synthetic materials, their IR spectra were taken by the KBr

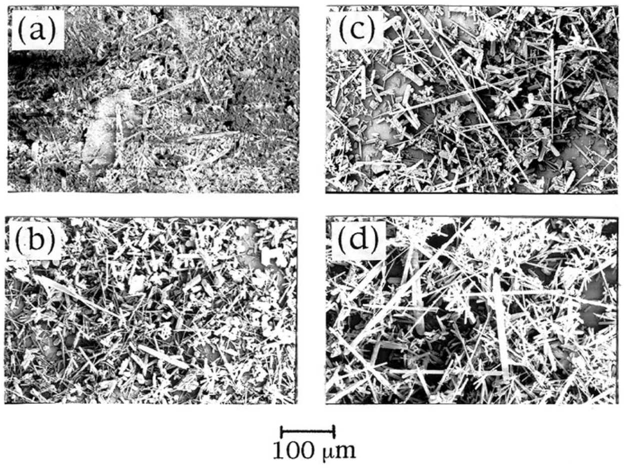

Fig. 4 SEM pictures of the materials formed at [AA] = 2.4 mol dm^{-3} and different t_a: (a) 6 h, (b) 6 days, (c) 16 days, (d) 26 days.

method. IR spectra of the particles formed at different [AA] and $t_a = 18$ days are depicted in Fig. 5. Spectrum (a) of $PbHPO_4$ particles shows broad weak bands. All the spectra except spectrum (a) show absorption bands at 1036, 982, 964, 575, 550 and 532 cm^{-1}, which are assigned to PbHAP.[3,8,16] The strong bands at 1036–964 cm^{-1} are assigned to the P–O stretching vibrations of PO_4^{3-} and three bands at 575, 550 and 532 cm^{-1} to the deformation vibrations of this ion.[8,16] No band shift with changing [AA] is observed in spectra (b)–(f). All the bands are diminished on decreasing [AA] from 4.8 to 0.2 mol dm^{-3}, caused by increased scattering of the IR beam by the larger particles formed at lower [AA]. Spectra (b)–(d) are characteristic of PbHAP and spectra (e) and (f) of a mixture of PbHAP and α-$Pb_3(PO_4)_2$, as confirmed by XRD (Fig. 1). The IR spectra of PbHAP and α-$Pb_3(PO_4)_2$

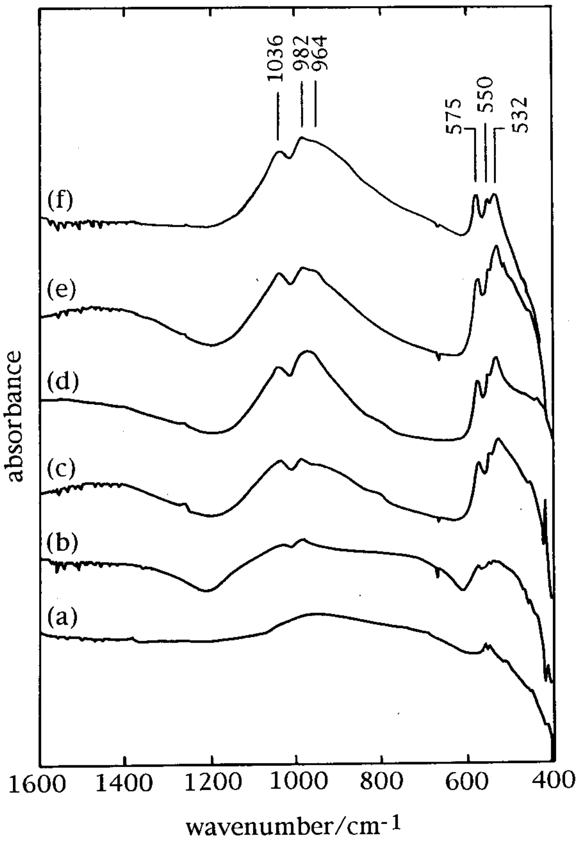

Fig. 5 IR spectra of the materials formed at $t_a = 18$ days and different [AA]: (a) 0.2, (b) 0.4, (c) 0.8, (d) 2.4, (e) 3.2, (f) 4.8 mol dm^{-3}.

resemble each other[8,16,17] and the amount of α-$Pb_3(PO_4)_2$ in the mixture is rather small as is clear from the XRD patterns (d) and (e) (Fig. 1) and the SEM pictures (e) and (f) (Fig. 3), so that it is hard to distinguish between pure PbHAP and a mixture with α-$Pb_3(PO_4)_2$ by IR spectroscopy alone.

TG–DTA curves

Thermal analyses were carried out to gain further insight into the structure of the products. Fig. 6 illustrates TG–DTA curves of the particles formed at different [AA] with $t_a = 18$ days. TG curve (a) of $PbHPO_4$ obtained at [AA] = 0.2 mol dm^{-3} shows a steep weight loss of 77 wt% at 190–370 °C. All the other samples give rise to a monotonous weight loss, continuing from room temperature to *ca.* 900 °C, accompanied by a broad DTA exothermic peak, due to release of adsorbed and/or bound water. TG curves (b)–(e) exhibit a small weight change at 953–997 °C related to melting of the particles, although these melting points are slightly lower than the literature value of 1000 °C.[8] PbHAP and the mixture of PbHAP and α-$Pb_3(PO_4)_2$ prepared in the present study showed similar TG and DTA curves because of the low α-$Pb_3(PO_4)_2$ content as mentioned above. The XRD pattern of PbHAP heated in air at 1100 °C for 2 h, taken at room temperature, was characteristic of α-$Pb_3(PO_4)_2$. All the samples obtained at [AA] = 2.4 mol dm^{-3} and $t_a = 1$–30 days exhibit essentially the same TG–DTA curves, although they are not given here except for curves (c) and (c′) of the particles prepared from the same solution at $t_a = 18$ days.

CaHAP particles prepared by the present method, using $Ca(NO_3)_2 \cdot 4H_2O$ instead of $Pb(NO_3)_2$ showed Ca/P molar ratios ranging widely from 1.44 to 1.70,[10] whereas the Pb/P ratios of all the PbHAP particles obtained in the present study are 1.59–1.67, nearer to the stoichiometric ratio of 1.67 than Ca/P ratios of the CaHAP particles. This result suggests that PbHAP particles containing nearly stoichiometric amounts of Pb can easily be prepared by the present method. It is frequently found that the TG curve of cation-deficient CaHAP possesses a steep weight loss at 750–900 °C, due to the following dehydration reaction [eqn. (2)], and an accompanying exothermic DTA peak.[18]

$$1/2\, P_2O_7^{4-} + OH^- \rightarrow PO_4^{3-} + 1/2\, H_2O \tag{2}$$

A similar reaction is expected to take place in PbHAP. However, a weight loss at 750–900 °C is not detected in the TG curves of PbHAP in Fig. 6. We can estimate the weight loss from the dehydration reaction (2) using the Pb/P molar ratios of the samples, as determined by chemical analysis. Since the Pb/P ratios of the particles showing TG curves (b) and (c) are respectively 1.63 and 1.67, their theoretical weight loss values by reaction (2) are 0.08 and 0 wt%, respectively. PbHAP prepared at [AA] = 2.4 mol dm^{-3} and $t_a = 14$ days shows a lowest ratio of 1.59 and the theoretical weight loss estimated from this ratio is 0.16 wt%, although its TG curve is not shown. However, such a small weight loss cannot be detected on the TG curves due to the sensitivity limits of the apparatus.

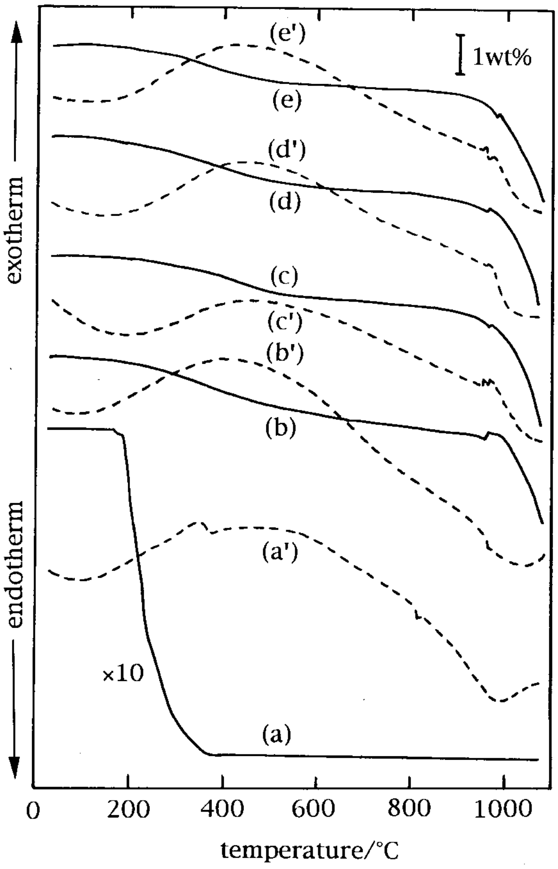

Fig. 6 TG (—) and DTA (· · ·) curves for the materials formed at $t_a = 18$ days and different [AA]: (a), (a′) 0.2; (b), (b′) 0.4; (c), (c′) 2.4; (d), (d′) 3.2; (e), (e′) 4.8 mol dm^{-3}. TG curve (a) is reduced to 10%.

Crystal phase

In order to determine the relationship between the crystal phase of the products and the synthetic conditions, particles were prepared by varying [AA] from 0.2 to 4.8 mol dm^{-3} and t_a from 6 h to 30 days. The crystal phases of the products, determined by XRD, are shown in Fig. 7. The products at [AA] = 0.2 mol dm^{-3} are $PbHPO_4$ regardless of t_a (open squares). The products at [AA] ≥ 0.4 mol dm^{-3} and $t_a = 6$ h are mixtures of PbHAP, α-$Pb_3(PO_4)_2$ and $PbHPO_4$ (solid circles). PbHAP can be synthesized at [AA] = 0.4–1.6 mol dm^{-3} and $t_a = 1$–30 days (open circles). Mixtures of PbHAP and α-$Pb_3(PO_4)_2$ are formed at [AA] ≥ 3.2 mol dm^{-3} and $t_a = 1$–30 days (open triangles). At [AA] = 2.4 mol dm^{-3} and $t_a = 1$–6 days, mixtures of PbHAP and α-$Pb_3(PO_4)_2$ are formed and pure PbHAP results at $t_a \geqslant 14$ days. These results indicate that the precipitated particles transform during ageing *via* the following reactions [eqn. (3), (4)]; at $t_a < 1$ day,

$$10\, PbHPO_4 + 2\, H_2O \rightarrow Pb_{10}(PO_4)_6(OH)_2 + 4\, H_3PO_4\text{[19,20]} \tag{3}$$

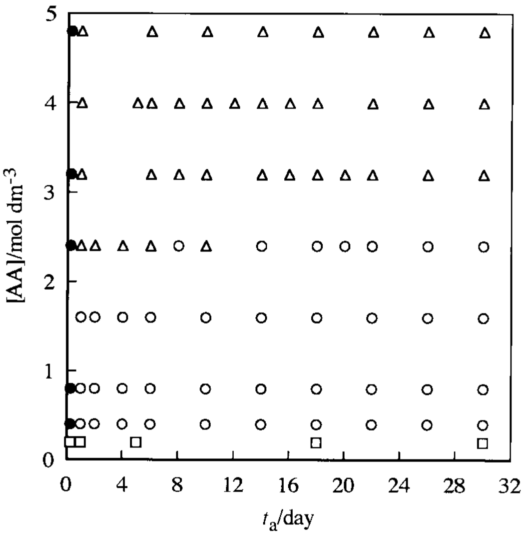

Fig. 7 The crystal phases of the materials obtained at different [AA] and t_a: (○) PbHAP, (△) PbHAP–α-$Pb_3(PO_4)_2$ mixture, (□) $PbHPO_4$, (●) PbHAP–α-$Pb_3(PO_4)_2$–$PbHPO_4$ mixture.

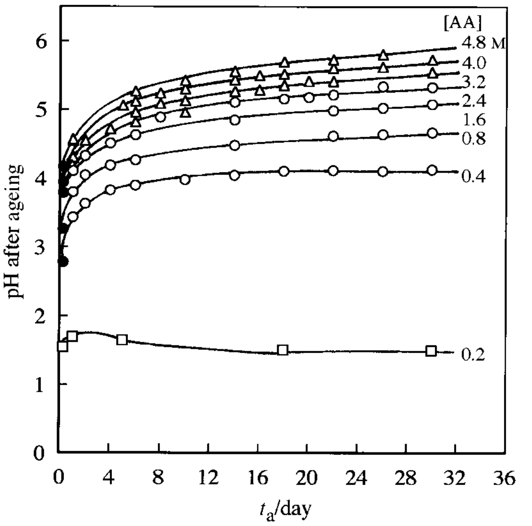

Fig. 8 The relationship between pH after ageing and t_a for materials formed at different [AA]: (○) PbHAP, (△) PbHAP–α-$Pb_3(PO_4)_2$ mixture, (□) $PbHPO_4$, (●) PbHAP–α-$Pb_3(PO_4)_2$–$PbHPO_4$ mixture.

and at $t_a = 1$–14 day,

$$10\,Pb_3(PO_4)_2 + 6\,H_2O \rightarrow 3\,Pb_{10}(PO_4)_6(OH)_2 + 2\,H_3PO_4\text{[19,20]} \tag{4}$$

The α-$Pb_3(PO_4)_2$ and $PbHPO_4$ particles are irregularly shaped, while the PbHAP particles are needle-like, as already mentioned. Consequently, PbHAP seems to be produced by transformation from α-$Pb_3(PO_4)_2$ and $PbHPO_4$ with an accompanying change in morphology.

pH Change by ageing

Fig. 8 shows the relationship between t_a and solution pH after ageing, where the symbols are the same as those used in Fig. 7. As [AA] increases from 0.2 to 4.8 mol dm^{-3}, the pH after ageing increases over the entire t_a range and continues to rise until $t_a = 30$ days except for the ageing at [AA] = 0.2 mol dm^{-3} (squares). Since CaHAP is known to be formed in alkaline or neutral environments, such as pH 8.5–9.5,[21] 8.5–11.0,[22] 6.0–9.0,[1] a similar result is anticipated for PbHAP, *e.g.* at pH 12[6] and 6.8.[7] Therefore, it should be noted that CaHAP and PbHAP can be produced by the present synthesis using AA at low pH, 4.59[10] and 3.43–5.33, respectively.

As mentioned in the introduction, AA hydrolyzes by reaction (1) to produce NH_3 which elevates the solution pH. When the solution pH rises sufficiently, precipitation starts to take place. At higher [AA], more NH_3 is generated elevating the solution pH more steeply. Simultaneously, more CH_3COOH is produced by hydrolysis of AA and is thought to interfere with PbHAP formation. To corroborate this effect, alternative preparations using NH_3(aq) and CH_3COOH were carried out under the conditions shown in Table 1 and were compared with the preparation using AA. Samples A1 and A2 were prepared at [AA] = 1.6 and 2.4 mol dm^{-3}, respectively, and $t_a = 2$ days and are included in Fig. 7. Samples C1 and C2 were synthesized by adding 17 mol dm^{-3} CH_3COOH solution to others containing NH_4NO_3, $Pb(NO_3)_2$, $(NH_4)_2HPO_4$ and HNO_3 at the concentrations shown in Table 1. For samples C1 and C2, the amounts of CH_3COOH added were estimated by assuming the hydrolysis of all the AA contained in the solutions of A1 and A2. After the addition of CH_3COOH, NH_3 (aq) solution was added to the reaction mixtures of C1 and C2 until the pH reached 4.33 and 4.55, respectively, the same as those of A1 and A2. For samples N1 and N2, NH_3 (aq) solution was added to the mixtures containing the reagents shown in Table 1 until the solution pH reached 7.36 and 7.20, respectively. This was done in order to adjust the solution pH after ageing to near those of A1 and A2. The volumes of all the solutions shown in Table 1 were adjusted to 250 cm^3 by adding water. After ageing at 100 °C for 2 days the particles were washed and dried as described in the experimental section. The solutions used for samples A1, C1 and N1 exhibited almost the same pH, 4.30–4.33, after ageing, while the solutions for samples A2, C2 and N2 showed pH 4.55–4.68. The crystal phases of the samples determined by XRD are given in Table 1. Samples A1, C1, N1 and N2 were PbHAP, while samples A2 and C2 were a mixture of PbHAP and α-$Pb_3(PO_4)_2$. It is clear from this result that the existence of more than 2.4 mol dm^{-3} CH_3COOH in the sample solution is related to the formation of a mixture of PbHAP and α-$Pb_3(PO_4)_2$. Consequently, in the synthesis of PbHAP using AA the transformation of α-$Pb_3(PO_4)_2$ to PbHAP is hindered by CH_3COOH generated by the hydrolysis of AA. Additionally, the formation of PbHAP particles depends not only on the solution pH but also the ageing period and the solution composition. The inhibition of calcium orthophosphate formation by di-, tri- and poly(carboxylic) acids has been reported.[23,24] Brecevic *et al.* found these anions hindered the growth of CaHAP crystals perpendicular to the (001) plane to produce needle-like particles and they explained this result by proposing that complexation of the Ca^{2+} ions by the carboxylic acids occurs.[23] Although the details of the inhibitory mechanism on PbHAP formation by CH_3COOH are unclear for the moment, an explanation similar to that used for the poly(carboxylic) acids can be predicted in the case of CH_3COOH.

Conclusion

Large needle-like highly crystalline PbHAP particles have been prepared by the homogeneous precipitation method using acetamide (AA). The PbHAP particles were obtained at [AA] = 0.4–1.6 mol dm^{-3} and $t_a \geq 1$ day. The CH_3COOH produced by the hydrolysis of AA interfered with the transformation of α-$Pb_3(PO_4)_2$ to PbHAP.

Table 1 Synthesis conditions and crystal phases of the products[a]

Sample	[HNO_3]/ mol dm^{-3}	[AA]/ mol dm^{-3}	[CH_3COOH]/ mol dm^{-3}	[NH_3 (aq)]/ mol dm^{-3}	pH before ageing	pH after ageing	Crystal phase by XRD
A1	0.28	1.6	—	—	0.92	4.33	PbHAP
C1	0.28	—	1.6	1.01	4.33	4.33	PbHAP
N1	0.28	—	—	0.34	7.36	4.30	PbHAP
A2	0.36	2.4	—	—	0.90	4.55	PbHAP + α-$Pb_3(PO_4)_2$
C2	0.36	—	2.4	1.35	4.55	4.55	PbHAP + α-$Pb_3(PO_4)_2$
N2	0.36	—	—	0.42	7.20	4.68	PbHAP

[a] The ageing temperature and period were 100 °C and 2 days; [NH_4NO_3] = 0.10 mol dm^{-3}, [$Pb(NO_3)_2$] = 0.05 mol dm^{-3}. [$(NH_4)_2HPO_4$] = 0.03 mol dm^{-3}.

Acknowledgements

The authors thank Mr. Masao Fukusumi of the Osaka Municipal Technical Research Institute for help with the TEM observations. This study was supported in part by the Nippon Sheet Glass Foundation and by the Grant-in-Aid for Science Research Funds (B) and (C) from the Ministry of Education, Science, Sports and Culture, Japanese Government.

References

1 J. C. Elliott, *Structure and Chemistry of the Apatites and Other Calcium Orthophosphates*, Elsevier, Amsterdam, 1994, p. 111.
2 Y. Matsumura, J. B. Moffat, S. Sugiyama, H. Hayashi, N. Shigemoto and K. Saitoh, *J. Chem. Soc., Faraday Trans.*, 1994, **90**, 2133.
3 G. Engel and W. E. Klee, *J. Solid State Chem.*, 1972, **5**, 28.
4 K. C. Blakeslee and R. A. Condrate, Sr., *J. Am. Ceram. Soc.*, 1971, **54**, 559.
5 T. Negas and R. S. Roth, *J. Res. Nat. Bur. Stand., Sect. A*, 1968, **72**, 783.
6 T. S. B. Narasaraju, R. P. Singh and V. L. N. Rao, *J. Inorg. Nucl. Chem.*, 1972, **34**, 2072.
7 R. Klement, *Z. Anorg. Allg. Chem.*, 1938, **237**, 161.
8 V. M. Bhatnagar, *Rev. Roum. Chim.*, 1971, **16**, 1513.
9 S. Sugiyama, T. Nakanishi, T. Ishimura, T. Moriga, H. Hayashi, N. Shigemoto and J. B. Moffat, *J. Solid State Chem.*, 1999, **143**, 296.
10 A. Yasukawa, H. Takase, K. Kandori and T. Ishikawa, *Polyhedron*, 1994, **13**, 3071.
11 T. Ishikawa, M. Wakamura and S. Kondo, *Langmuir*, 1989, **5**, 140.
12 T. Ishikawa, M. Wakamura, T. Kawase and S. Kondo, *Langmuir*, 1991, **7**, 596.
13 T. Ishikawa and S. Kondo, in *Fundamentals of Adsorption*, ed. A. B. Mersman and S. E. Scholl, Engineering Foundation, New York, 1991, p. 321.
14 S. J. Joris and C. H. Amberg, *J. Phys. Chem.*, 1971, **75**, 3167.
15 R. C. Rau, *Norelco Rep.*, 1963, **10**, 114.
16 W. E. Klee and G. Engel, *J. Inorg. Nucl. Chem.*, 1970, **32**, 1837.
17 R. A. Nyquist and R. O. Kagel, in *Infrared Spectra of Inorganic Compounds*, Academic Press, New York, 1971, p. 169.
18 J. A. S. Bett, L. G. Christner and W. K. Hall, *J. Am. Chem. Soc.*, 1967, **89**, 5535.
19 R. W. Mooney and M. A. Aia, *Chem. Rev.*, 1961, **61**, 433.
20 T. Kanazawa, *Inorganic Phosphorus Chemistry*, Kodansha, Tokyo, 1985, p. 164.
21 E. C. Moreno, T. M. Gregory and W. E. Brown, *J. Res. Nat. Bur. Stand., Sect. A*, 1968, **72**, 773.
22 H. Monma, *Shokubai*, 1985, **27**, 237.
23 L. Brecevic, A. Sendijarevic and H. Furedi-Milhofer, *Colloids Surf.*, 1984, **11**, 55.
24 Z. Amjad, *J. Colloid Interface Sci.*, 1987, **117**, 98.

Paper 9/00758J